This full text paper was peer reviewed at the direction of IEEE Communications Society subject matter experts for publication in the WCNC 2008 proceedings.

# Intelligent Weather Systems with Fuzzy Logic Controller for Satellite Networks

Kamal Harb[1,2], Changcheng Huang[2], Anand Srinivasan[1] and Brian Cheng[1]
1 – EION Wireless, 320 March Rd, Suite 500, Ottawa, Ontario, Canada K2K 2E3
2 – Carleton University, 1125 Colonel By Drive, Ottawa, Ontario, Canada K1S 5B6
Email: kharb@sce.carleton.ca

***Abstract*— Weather attenuations can have a distorting effect on signal fidelity above 10 *GHz* that lead to excessive digital transmission error. This loss of signal is commonly referred to as signal attenuation. Signal attenuation impacts QoS in wireless and satellite networks. An intelligent decision support system is therefore necessary for service providers by accurately calculating rain, gaseous, cloud, fog, and scintillation attenuations using predicted signal-weather correlated database in collaboration with ITU-R propagation models combined with gateway, and ground terminal characteristics. The effect becomes a key feature in adjusting and improving satellite signal power, modulation and coding schemes, monitored and controlled altogether by a powerful and efficient intelligent-based attenuation countermeasure system. A three dimensional relationship is proposed among these attenuations with respect to propagation angle and rainfall rate [1]-[9]. The result pilots an enhanced back propagation-learning algorithm that is used to iteratively tune the intelligent controller based on fuzzy logic technique with returned SNR values for activating the weighted Modulation/ Codepoint to its optimal values, depending on actual or predicted weather conditions, configuration settings and tolerance/safety margins for SLA commitment.**

***Index Terms* — Intelligent System (IS), International Telecommunications Union - Radiocommunications (ITU-R), Quality of Service (QoS), Rain Attenuation (RA), and Service Level Agreements (SLA), Signal to Noise Ratio (SNR).**

## I. INTRODUCTION

Propagation impairments include various attenuations, which affect satellite links above Ku bands. RA is considered a dominant impairment for satellite signals becomes particularly severe at frequencies higher than 10 *GHz* [7]-[8].

A number of prediction models are available for estimating individual components. However, methodologies that attempt to combine them in a cohesive manner are not widely available yet [10]. Furthermore, it is extremely hard to optimally manage satellite-available network resources that are impacted by attenuations, with link traffic engineering only - “Goldilocks Link Budgeting”. It is then absolutely necessary to correctly identify and predict the overall impact of every significant attenuation factors on QoS [11]-[13].

In the absence of detailed knowledge of occurrence probabilities for different impairments, empirical approaches are taken by estimating their combined effects. Once the amounts are established, appropriate methods for mitigating impairments must be invoked. Some of these include adaptive coding, antenna beam shaping, site diversity, and up-link power control. Notice that, Up-link power control is one of the most cost-effective attenuation mitigation techniques. It enhances link availability and performance [11]-[15].

In view of these analytical approaches, dealing with weather-impacted QoS and reliable satellite communications are currently non-existent. Other thrusts in satellite service providers are shifting their resolution towards intelligent-based prediction methods. They predict relevant atmospheric metrics accurately by adaptively applying these methods to regulate transmit power, transmission rate, modulation schemes and channel coding. As a result, new received signal promptly changes by adjusting the inter-connected network entities, before unpredicted forecasts actually manifest themselves, to maintain end-to-end QoS requirements.

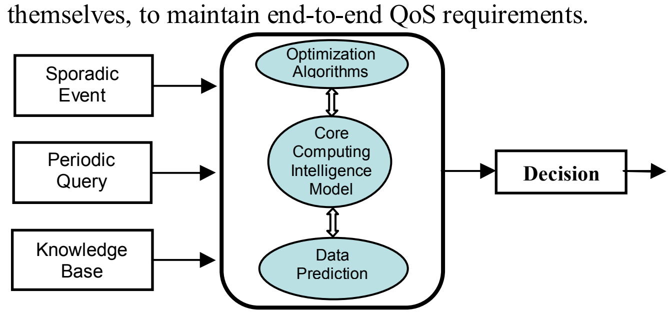


**Fig. 1.** Network Optimization Decision Support System

Fig. 1 shows the high level architecture of the network optimization decision support system. Weather attenuation, power, modulation, and coding information are used to obtain optimal decision.

The work presented in this paper fits in the data prediction module and the interface to the core computing intelligence model of the decision support system.

We use ITU-R models to accurately compute rain, gaseous, cloud, fog and scintillation attenuations as a function of both propagation angle and rainfall rate [1]. This data controlled by the intelligent system via a Fuzzy Logic decision mechanism, provide a better estimate satellite networking parameters such as link and queuing characteristics. The derived parameters would enable the IS to maintain QoS and SLAs.

The remaining sections of this paper are as follows: In section II, we calculate rain, gaseous, scintillation, cloud, and fog attenuations. It is then followed by a simulation and analysis of atmospheric attenuation. In sections III and IV, SNR estimation and intelligent signal for satellite system are presented. Finally, conclusion is outlined in section V.

## II. DIFFERENT ATTENUATIONS CALCULATION

### *II. 1 Rain Attenuation*

Long-term statistics of slant-path RA for any given location at

This full text paper was peer reviewed at the direction of IEEE Communications Society subject matter experts for publication in the WCNC 2008 proceedings.

frequencies up to 55 *GHz* is provided using ITU-R estimates. With respect to altitude where rainfall rate ($R_p$) extends during periods of precipitation as described in [1] and [4], RA's behaviour can be computed for any location and any frequency, based on frequency sample ($F_i$), as follows:

*1)*- If no specific information is available: the mean 0℃ isotherm height - with resolution of 1.5° in both latitude and longitude - above mean sea level $h_0$ could be obtained from ITU-R data file *HEIGHT0.txt* [6].

*2)*- Mean rain height above mean sea level, $h_R$, can be obtained from 0℃ isotherm $h_0$ as: $h_R = h_0 + 0.36 \ km.$ (1)

*3)*- To compute slant-path length, $L_S$, below rain height, the following formulas are used, where $R_e$: radius of Earth (*km*):

i- $\theta < 5°$: $$L_S = \frac{2(h_R - h_S)}{\left(\sin^2\theta + \frac{2(h_R - h_S)}{R_e}\right)^{1/2} + \sin\theta} \ km \quad (2a)$$

ii- $\theta \geq 5°$: $$L_S = \frac{(h_R - h_S)}{\sin\theta} \ km \quad (2b)$$

if $(h_R - h_S) \leq 0 \Rightarrow$ predicted RA for any time percentage is equal to zero and the following steps are not required.

*4)*- Calculate horizontal projection, $L_G$, of slant-path length from: $L_G = L_S \cos\theta \ km$ (3)

*5)*- Find rainfall rate, $R_p$, for exceeded $p = 0.01\%$ of an average year. If $R_{0.01} = 0 \Rightarrow RA = 0$ for any time percentage and the following steps are not required [1].

*6)*- Compute specific attenuation, $\gamma_R$, using frequency-dependent coefficients as given in [3] for $k$, $\alpha$ and $R_p$ for $p = 0.01\%$ by using: $\gamma_{0.01} = K \ (R_{0.01})^{\alpha} \ dB/km$ (4)

For linear and circular polarization and for all path geometries, coefficients in (4) can be computed from (5) and (6) as:

$$K = \left[K_H + K_V + (K_H - K_V)\cos^2\theta\cos 2\tau\right]/2 \quad (5)$$

$$\alpha = \left[K_H\alpha_H + K_V\alpha_V + \left(K_H\alpha_H - K_V\alpha_V\right)\cos^2\theta\cos 2\tau\right]/2k \quad (6)$$

where $K_V, \alpha_V$ and $K_H, \alpha_H$ are constant coefficients of vertical and horizontal polarizations respectively. Also, $\theta$ is the path propagation angle and $\tau$ is the polarization tilt angle relative to the horizontal, equal to 45 *degree* for circular polarization.

*7)*- Calculate horizontal reduction factor, $r_p$, for $p = 0.01\%$ :

$$r_{0.01} = \frac{1}{1 + 0.78\sqrt{\frac{L_G \cdot \gamma_{0.01}}{f}} - 0.38\left(1 - e^{-2L_G}\right)} \quad (7)$$

*8)*- Calculate vertical adjustment factor, $v_p$, for $p = 0.01\%$ :

$$\sigma = \tan^{-1}\left(\frac{h_R - h_S}{L_G \cdot r_{0.01}}\right) \ degrees \quad (8)$$

For $\sigma > \theta$, the actual slant-path length $L_R$ will be:

$$L_R = \frac{L_G \cdot r_{0.01}}{\cos\theta}, \text{ else } L_R = \frac{(h_R - h_S)}{\sin\theta} \ km \quad (9)$$

if $|\rho_e| < 36° \Rightarrow \chi = 36 - |\rho_e|$, else $\chi = 0$ *degree* (10)

$$v_{0.01} = \frac{1}{1 + \sqrt{\sin\theta}\left(31\left(1 - e^{-\left(\theta/(1+\chi)\right)}\right)\frac{\sqrt{L_R \cdot \gamma_{0.01}}}{f^2} - 0.45\right)} \quad (11)$$

*9)*- Effective path length is: $L_E = L_R \cdot v_{0.01} \ km$ (12)

*10)*- Predicted exceeded RA for $p = 0.01\%$ of an average year is obtained from: $A_{0.01} = \gamma_{0.01} \cdot L_E \ dB$ (13)

*11)*- For other exceeding percentages of an average year ranging from 0.001% to 5%, estimations of RA can be computed from (13) for an average year as follows:

if $p \geq 1\%$ *or* $|\rho_e| \geq 36° \Rightarrow \beta = 0$,

else if $p < 1\%$ *or* $|\rho_e| < 36°$ *and* $\theta \geq 25° \Rightarrow \beta = -0.005(|\rho_e| - 36)$,

otherwise $\beta = -0.005(|\rho_e| - 36) + 1.8 - 4.25\sin\theta$ (14)

$$A_{rain}(p) = A_{0.01}\left(\frac{p}{0.01}\right)^{-(0.655 + 0.033\ln(p) - 0.045\ln(A_{0.01}) - \beta(1-p)\sin\theta)} \ dB \quad (15)$$

Note: RA equation was tested by ITU-R and found to have the most accurate overall results of all tested models [1]-[9].

We propose to compute RA as a function of any frequency ($f$) value as: $A_{rain}(f_n) = \gamma_R(f_n) \cdot L_E(f_n) \ dB$ (16)

Also, for any specific frequency ranging from 7 to 55 *GHz* is obtained from:

$$H(\varphi(f_{n-1}), \varphi(f_n), A_{rain}(f_{n-1})) = 1.12\times10^{-3}\ldots$$
$$\cdot\left(\varphi(f_n)/\varphi(f_{n-1})\right)^{0.5}\left(\varphi(f_{n-1})A_{rain}(f_{n-1})\right)^{0.55} \quad (17)$$

$$A_{rain}(f_n) = A_{rain}(f_{n-1}) \cdot \left(\varphi(f_n)/\varphi(f_{n-1})\right)^{(1 - H(\varphi(f_{n-1}), \varphi(f_n), A_{rain}(f_{n-1})))} \ dB \quad (18)$$

where $A_{rain}(f_{n-1})$ and $A_{rain}(f_n)$ are the equiprobable values of excess RA at frequencies ($f_{n-1}$) and ($f_n$), respectively [1].

Methods explained so far, are used to investigate the dependence of RA statistics on propagation angle, rainfall rate, polarization, probability and frequency. Thus, if reliable attenuation data measured at any specific frequency is available, the adjusted empirical formulas shown in (16)-(18) will then provide RA as a function of its preceding frequency. That is, once we have RA at any lower frequency, we can then compute RA of upper level based on the obtained one and so on until we reach the maximum desired frequency [1] and [4]. Moreover, this method provides high CPU efficiency since we do not have to repeat the entire calculation from (4) for each frequency, as is the case of existing solutions [9]. Also, this paper introduces RA in (19) as a function of propagation angle ($\theta$) and rainfall rate ($R_p$), as shown in Fig. 1, by combining several equations: $A_{rain}(\theta, R_p) = \gamma_R(\theta, R_p) \cdot L_E(\theta, R_p) dB$ (19)

This method provides a useful general tool for scaling RA according to these parameters. Also, this model helps to provide designers with a perceptible view of approximate RA

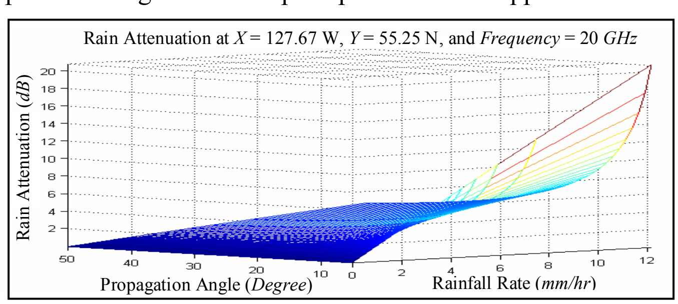


**Fig. 1.** Rain Attenuation at Hazelton Station

values that can be computed at any desired location (*X* and *Y*), for a different propagation angle ($\theta$), for any rainfall rate ($R_p$), and for any uplink or downlink frequencies ($f$).

### *II.2 Gaseous Attenuation*

In this section, analytical solution is presented to calculate attenuation due to atmospheric gases. Thus, predicting gaseous attenuation requires an accurate model that allows us to represent the specific attenuation mathematically. It can be calculated by summing the effects of all the significant resonance lines, as given in ITU-R P.676 and shown in Fig. 2:

*1- Specific Attenuation:*

A- For dry air, the attenuation $\gamma_0$ (*dB/km*) is given by the following equation for the frequency of interest ($f \leq 54$ *GHz*):

$$\gamma_o = \left[ \frac{7.2\, r_t^{2.8}}{f^2 + 0.34\, r_p^2\, r_t^{1.6}} + \frac{0.62\, \xi_3}{(54 - f)^{1.16\xi_1} + 0.83\, \xi_2} \right] f^2 r_p^2 \times 10^{-3} \quad (20)$$

with: $\xi_1 = \varphi(r_p, r_t, 0.0717, -1.8132, 0.0156, -1.6515)$ (21a)

$$\xi_2 = \varphi(r_p, r_t, 0.5146, -4.6368, -0.1921, -5.7416) \quad (21b)$$

$$\xi_3 = \varphi(r_p, r_t, 0.3414, -6.5851, 0.2130, -8.5854) \quad (21c)$$

$$\varphi(r_p, r_t, a, b, c, d) = r_p^a r_t^b \exp[\, c(1 - r_p) + d(1 - r_t)] \quad (22)$$

B- For water vapour, the attenuation $\gamma_W$ (*dB/km*) is given by:

$$\gamma_w = \left\{ \frac{3.98\eta_1 \exp[2.23(1-r_t)]}{(f-22.235)^2 + 9.42\eta_1^2} g(f,22) + \frac{11.96\eta_1 \exp[0.7(1-r_t)]}{(f-183.31)^2 + 11.14\eta_1^2} + \frac{0.081\eta_1 \exp[6.44(1-r_t)]}{(f-321.226)^2 + 6.29\eta_1^2} + \frac{3.66\eta_1 \exp[1.6(1-r_t)]}{(f-325.153)^2 + 9.22\eta_1^2} + \frac{25.37\eta_1 \exp[1.09(1-r_t)]}{(f-380)^2} + \frac{17.4\eta_1 \exp[1.46(1-r_t)]}{(f-448)^2} + \frac{844.6\eta_1 \exp[0.17(1-r_t)]}{(f-557)^2} g(f,557) + \frac{290\eta_1 \exp[0.41(1-r_t)]}{(f-752)^2} g(f,752) + \frac{8.3328\times 10^4 \eta_2 \exp[0.99(1-r_t)]}{(f-1\,780)^2} g(f,1\,780) \right\} f^2 r_t^{2.5} \rho \times 10^{-4} \quad (23)$$

with $\eta_1 = 0.955 r_{ph} r_t^{0.68} + 0.006\rho, \eta_2 = 0.735 r_{ph} r_t^{0.5} + 0.0353 r_t^4 \rho$ (24)

and $g(f, f_i) = 1 + \left( \frac{f - f_i}{f + f_i} \right)^2$ (25)

where *ph*: pressure (*hPa*), $r_p = ph/1013$, $r_t = 288/(273 + t)$, ρ: water-vapour density (*g/m³*), *f*: frequency (*GHz*), and *t*: mean temperature values (℃), can be obtained from ITU-R P.1510 when no adequate temperature data is available.

*2- Slant* Path *Equivalent Height:*

The slant path attenuation depends on the distribution along the path of meteorological parameters such as temperature, pressure, and humidity. Thus, it varies with location, time, height of station above sea level, and propagation angle.

A- For dry air, the equivalent height is given by:

$$h_o = \frac{6.1}{1 + 0.17\, r_p^{-1.1}} (1 + t_1 + t_2 + t_3) \quad (26)$$

with the constraint that: $h_o \leq 10.7\, r_{ph}^{0.3}$ when $f < 70$ *GHz*.

where: $t_1 = \frac{4.64}{1 + 0.066 r_{ph}^{-2.3}} \exp\left[ -\left( \frac{f - 59.7}{2.87 + 12.4 \exp(-7.9\, r_{ph})} \right)^2 \right]$, (27a)

$$t_2 = \frac{0.14 \exp(2.12\, r_{ph})}{(f - 118.75)^2 + 0.031 \exp(2.2\, r_{ph})}, \quad (27b)$$

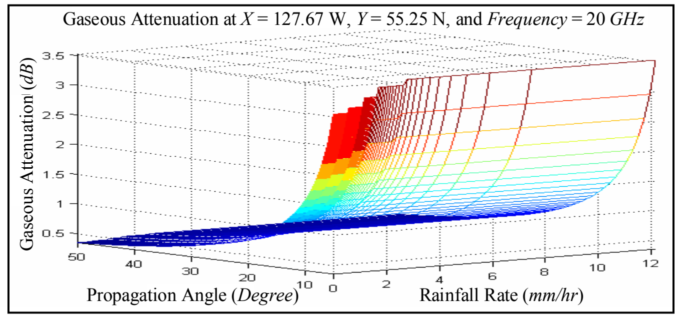


**Fig. 2.** Gaseous Attenuation at Hazelton Station

and $t_3 = \frac{0.0114}{1 + 0.14 r_{ph}^{-2.6}} f \frac{-0.0247 + 10^{-4} f + 1.61\times 10^{-6} f^2}{1 - 0.0169 f + 4.1\times 10^{-5} f^2 + 3.2\times 10^{-7} f^3}$ (27c)

B- for water vapour, the equivalent height for $f \leq 350$ *GHz* is:

$$h_w = 1.66\left( 1 + \frac{1.39\sigma_w}{(f - 22.235)^2 + 2.56\sigma_w} + \frac{3.37\sigma_w}{(f - 183.31)^2 + 4.69\sigma_w} + \frac{1.58\sigma_w}{(f - 325.1)^2 + 2.89\sigma_w} \right) \quad (28)$$

Notice that water vapour has resonance at (22.235), (183.31) and (325.1) *GHz* respectively and that attenuation changes with the amount of water vapour in the atmosphere.

*3- Path Attenuation for Earth-Space propagation angle between 5 and 70 degree*:

The above method calculates slant path attenuation of water vapour that relies on the knowledge of the profile of water-vapour pressure (or density) along the attenuation path. It provides useful general tools for scaling Gas according to these parameters. Thus, the approximate Gaseous values can be computed at any desired location (*X* and *Y*) and for a given uplink or downlink frequencies (*f*) as shown in Fig. 2.

This paper proposes to obtain the path attenuation based on surface meteorological data using the cosecant law for all ranges of propagation angle and rainfall rate, by combining several equations as: $A_{Gas}(\theta, R_p) = \frac{A_o + A_w}{\sin\theta}$ *dB* (29)

where $A_o = h_o\, \gamma_o$ and $A_w = h_w\, \gamma_w$ (30)

### *II.3 Clouds and Fog Attenuations*

Clouds and fog can be described as collections of smaller rain droplets or alternatively, as different interactions from rain as the water droplet size in fog and clouds is smaller that the wavelength at 3–30 *GHz*. These attenuations can be expressed in term of the rainfall rate and propagation angle for a specific frequency and temperature values, as shown in Fig. 3:

$$D_{p1} = ((\varepsilon_0 - \varepsilon_1)/(1 + (f/f_p)^2)) + ((\varepsilon_1 - \varepsilon_2)/(1 + (f/f_s)^2)) + \varepsilon_2 \quad (31a)$$

$$D_{p2} = (f.(\varepsilon_0 - \varepsilon_1)/(f_p.(1 + (f/f_p)^2))) + (f.(\varepsilon_1 - \varepsilon_2)/(f_s.(1 + (f/f_s)^2))) \quad (31b)$$

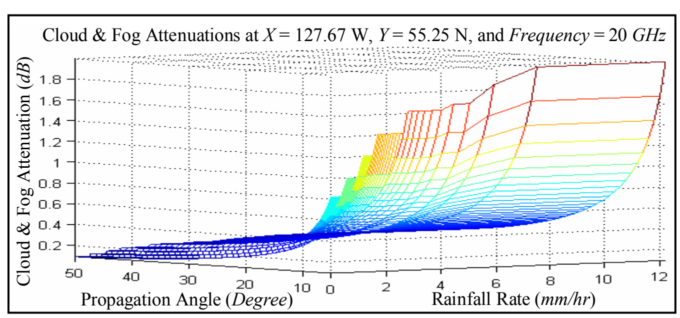


**Fig. 3**. Clouds and Fog Attenuations at Hazelton Station

$\eta = (2 + D_{p1}) / D_{p2}$ (32)

$K_l = (0.819 * f) / (D_{p2}. (1+ \eta^2))$ (33)

$t_1 = 300 / t_k$, where $t_k$ = Temperature (*Kelvin*) (34)

$\varepsilon_2 = 3.51$, $\varepsilon_1 = 5.48$, and $\varepsilon_0 = 77.6 + 103.3\ (t_1\text{-}1)$ (35)

$f_s = 590\text{-}1500(t_1\text{-} 1)$, and $f_p = 20.09 - 142(t_1\text{-}1) + 294(t_1\text{-}1)^2$ (36)

To obtain the predicted attenuation due to clouds for a given probability value, the statistics of the total columnar content of liquid water $L_w$ ($kg/m^2$), which is an integration of liquid water density, $M$ ($kg/m^3$), along a cross section of 1 $m^2$ from surface to top of clouds for a given site, must be known yielding as shown in Fig. 3 for propagation angle ranging between $90° \geq \theta \geq 5°$ as: $A_{Cloud\ \&\ Fog}(\theta, R_p) = \dfrac{L_w . K_t}{\sin\theta}\ dB$ (37)

*II.4 Scintillation Attenuation*

The cumulative distribution of tropospheric scintillation is based on monthly or longer average surface of ambient temperature $t$ (℃). This distribution reflects the specific climate conditions of the site [16]. Following is a general technique for predicting it at different rainfall rate and propagation angle that is greater than 4 ℃ is shown in Fig. 4.

Calculate the standard deviation of the signal amplitude, $\sigma_{ref}$, used as reference: $\sigma_{ref} = 3.6 . 10^{-3} + 10^{-4} . N_{wet}\ dB$ (38)

where $N_{wet}$: radio refractivity, given in ITU-R P.453.

Calculate the effective path length $L$ for $h = 1000\ m$:

$$L = \frac{2h}{\sqrt{\sin^2\theta + 2.35 \times 10^{-4}} + \sin\theta}\ m \quad (39)$$

$h_L$: the height of the turbulent layer equal to 1000 *m.*

Estimate the effective antenna diameter, $D_{eff}$, from the geometrical diameter ($m$) of the earth-station antenna, $D$, and the antenna efficiency $\eta$: if unknown, $\eta = 0.5$ is used as:

$$D_{eff} = \sqrt{\eta}\ .\ D\ \ meter \quad (40)$$

Calculate the antenna-averaging factor from:

$$g(x) = \sqrt{3.86\,(x^2+1)^{11/12} . \sin\left[\frac{11}{6}\arctan\frac{1}{x}\right] - 7.08\, x^{5/6}} \quad (41)$$

with $x = 1.22\ .\ D^2 eff\ .\ (f\ /L\ )$ (42)

$$\sigma = \sigma_{ref}\ .\ f^{7/12}\ .\ \frac{g(x)}{(\sin\theta)^{1.2}} \quad (43)$$

where $f$ is the carrier frequency ranges from 4 to 30 *GHz*.

Calculate time percentage factor, $a(p)$, for the probability of attenuation ($p$) being exceeded ranges from 0.001% to 50% as:

$a(p) = -0.061.(\log p)^3 + 0.072.(\log p)^2 - 1.71.\log(p) + 3.0$ (44)

Calculate the scintillation fade depth as:

$A_{Scintillation}\ (\theta,\ p) = a\ (p)\ \cdot\ \sigma(\theta)\ \ dB$ (45a)

It can also be written after mathematical manipulation as:

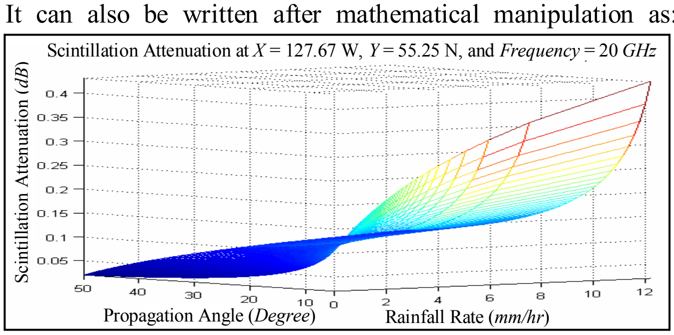


**Fig. 4.** Scintillation Attenuation at Hazelton Station

$A_{Scintillation}\ (\theta,\ R_p) = a\ (p)\ \cdot\ \sigma(\theta)\ dB$ (49b)

*II.5 Atmospheric Attenuation*

In this section we calculate atmospheric attenuation based on rain, gas, cloud, fog and scintillation attenuations as per Fig. 5. These attenuations for systems operating at frequencies above 10 *GHz* [13] - especially those operating with low propagation angles and/or margins - must be considered along with the effect of multiple sources of simultaneous occurring.

The required input parameters for the above attenuations are:

$A_{Rain}(\theta, R_p)$: attenuation due to rain, as estimated in (19).

$A_{Gas}(\theta, R_p)$: gaseous attenuation due to water vapour and oxygen, as estimated in (29).

$A_{Cloud\&Fog}\ (\theta, R_p)$: cloud and fog attenuation, as per in (37).

$A_{Scintillation}(\theta, R_p)$: attenuation due to tropospheric scintillation, as estimated by (45).

A general method for calculating total attenuation for a given propagation angle and Rainfall rate, $A_W\ (\theta, R_p)$, is given by:

$$A_W = A_{Gas} + \sqrt{\left(A_{Rain} + A_{Cloud\ \&Fog}\right)^2 + A_{Scintillation}^{\ 2}}\ dB \quad (46)$$

where $A_{cloud\&Fog}(\theta, R_p) \cong A_{cloud\&Fog}(\theta, R_{1\%})$ for $p < 1.0\%$ (47a)

and $A_{Gas}\ (\theta, R_p) \cong A_{Gas}\ (\theta, R_{1\%})$ for $p < 1.0\ \%$ (47b)

Equations (47a) and (47b) take into consideration that a large part of cloud and gaseous attenuations are already included in RA prediction for time percentage below 1% [9].

This prediction method was tested using contour rain map in [3], and procedures set out in ITU-R P.311. The results were found to be in good agreement with the available measurement data for all latitudes for the probability ranging from 0.001% to 1% with an overall r.m.s. error about 35%. Whereas, the overall r.m.s. error was found to be about 25% when using multi-year Earth-space data.

Therefore, due to the dominance of different effects at different probabilities as well as the inconsistent availability of test data at different probability levels, some variations of r.m.s. errors occur across the distribution of different probabilities. Thus, knowing this data will be an immense asset to support analysis for budgeting the operational satellite networking parameters around the world.

## III. SIGNAL TO NOISE RATIO (SNR) CALCULATION

By definition, SNR is a measure of signal strength for satellite signal relative to attenuations and background noise. Based on previous calculations for different attenuations, we are able to estimate SNR accurately. SNR is usually measured in decibels ($dB$) and is calculated as follows [15]:

Thermal noise power Spectral density is: $N_0 = K\ .\ T$ where $K = 1.38.10^{-23}\ Ws/K = -228.6\ dB\ Ws/K$ and

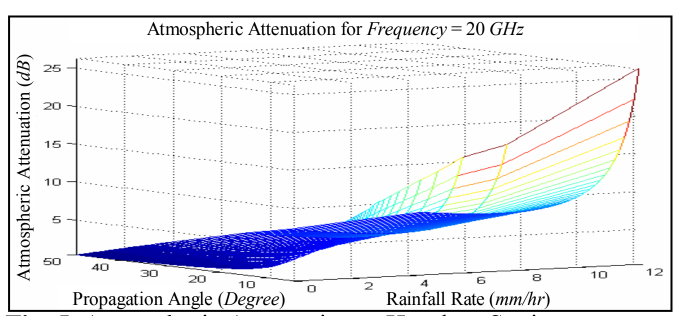


**Fig. 5.** Atmospheric Attenuation at Hazelton Station

$T$ (*effective noise temperature*) = $T_a + T_r$ Consequently, $T_r$ (*Noise temperature of the Receiver*) $= (10^{N_r/10} - 1).290$ (48)
where noise figure of Low-noise amplifier, $N_r \approx 0.7$ - 2 *dB*. $T_a$ Noise temperature of the Antenna is represented in Table 1. Thus, ratio between signal and noise power spectral density is:

$$\frac{C}{N_0} = \frac{C}{K\,.\,T} = \frac{P_r}{K\,.\,T} \ldots \tag{49a}$$

$$\ldots = \frac{P_t\,.\,G_t}{A_t}\,.\,\frac{G_r}{K\,.\,T} = \frac{EIRP}{A_t}\,.\,\frac{G_r}{K\,.\,T}$$

$$\left.\frac{C}{N_0}\right|_{dB} = P_t + G_t - A_t + G_r - K - T \tag{49b}$$

**Table 1.** Noise Temperature in Antenna

| Antenna Noise temperature Ta (*Kelvin*) | | |
|---|---|---|
| Directional satellite antenna | Earth from space | 290 *K* |
| Directional terminal antenna | Space from earth at 90˚elev.<br>Space from earth at 10˚elev.<br>Sun (1…10 *GHz*) | 3 – 10 *K*<br>≈ 80 *K*<br>$10^5$….$10^4$ *K* |
| Hemispherical terminal antenna | At night<br>Cloudy sky<br>Clear sky with sunshine | 290 *K*<br>360 *K*<br>400 *K* |

Where $A_t$ (*total attenuation*) = $A_W + A_0$ (*free space loss*), such as $A_0 = (4.\pi.d/\lambda)^2$, $d$ = distance between transmitter and receiver, $\lambda$(*wavelength*) = $c/f$ , $P_t$ and $P_r$ are transmitted and received power, and $G_t$ and $G_r$ are antenna gain at transmitter and receiver sides respectively. By considering a receive filter with noise of equivalent bandwidth ($B_r$), the noise power $N$ will be: $N_0\,.\,B_r = K\,.\,T\,.\,B_r$, and

Therefore, $SNR = \frac{C}{N} = \frac{C}{N_0}\,.\,\frac{1}{B_r}$ *dB* (50)

## IV. Signal to Noise Ratio modification

Several factors such as power, modulation, etc., can perform an immense role in improving SNR and in maximizing system throughput and availability of the link. In this section, a new proposed method, shown in Fig. 6, is introduced to overcome different weather conditions. Thus, by controlling the above mentioned factors that supply the fuzzy logic mechanism, to allow better estimates for satellite networking parameters such as link and queuing characteristics. These derived parameters adaptively adjusting signal power, coding, modulation, and would enable the proposed system to maintain SNR by transmission rate under unpredictable forecast.

By definition, $E_s$ (*symbol energy*) = $C\,.\,T_s = C / R_s$, where

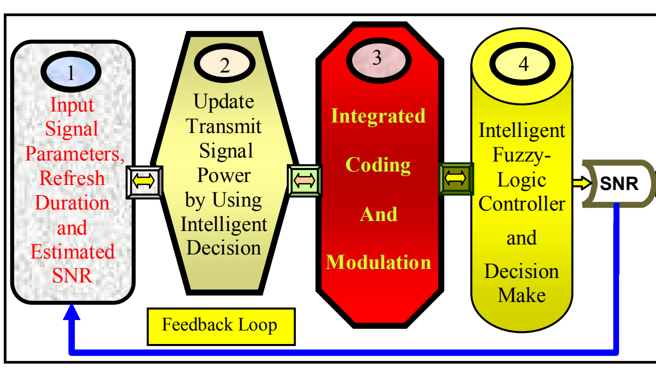


**Fig. 6.** Intelligent Fuzzy Weather Controller

transmission rate $R_s$ (*symbol/sec*) is inversely equivalent to $T_s$ (*symbol duration*) = $1/R_s$ and symbol energy-to-noise power density is: $\frac{E_s}{N_0} = \frac{C}{N_0}\,.\,T_s$ , where:

$$\frac{E_s}{N_0} = \frac{C}{N_0}\,.\,\frac{1}{R_s} \quad \text{or} \quad \left.\frac{E_s}{N_0}\right|_{dB} = \frac{C}{N_0} - R_s \tag{51a}$$

$$\left.\frac{E_s}{N_0}\right|_{dB} = P_t + G_t - A_t + G_r - T - K - R_s \; dB \tag{51b}$$

$E_s / N_0$: Can be used to determine the bit error rate of a digital transmission scheme, or visa versa.

Fig. 6 illustrates a manner for changing parameters of the communication system in order to overcome the deteriorating effect of atmospheric impairments, and to increase reliability of the data transmitted throughout the channel. In the first stage, the system holds input signal parameters such as frame size, propagation angle, etc. and SNR estimated values that were compared against threshold level, in a single database. The result should be greater than or at least equal to this level.

In the second stage, based on SNR values, either the intelligent system will decide to increase transmit power for a maximum limit of -30 *dB* (0 *dBm*), or to skip to the next stage. Next, SNR value will be checked among modulation and coding values given in Table 2. If this value can be reached by using any of the mentioned table combinations, then the system will go to the final stage.

In the last stage, the system will compromise among different SNR achieved outputs and make decision based on the intelligent fuzzy logic controller according to available parameters and requirements. The given feedback will keep looping until a satisfactory value is reached.

Thus, this system can also change data rate, frame size, frequency, etc. in order to adjust SNR in cases such as unpredicted bad weather condition by using refresh duration that is located in the first stage.

Fig. 7 and Fig. 8 compared the outputs of SNR ranges before and after modification respectively. Where SNR used to fall between (-51 ~ -28) *dB*, for power transmits from (-98 ~ -88) *dB*, and was transformed after intelligent decision mechanism to fall within modulation and coding boundaries of allowable used database. The adjusted output for SNR ranges from (-1.5 ~ 22) *dB*, (-48 ~ -38) *dB* for transmitted power, and (0 ~ 13.0) *mm/hr* for unchanged rainfall rate in both results.

Note that, there is a limit of increasing transmits power up to around –30 *dB*. Once this value has been reached, Mod/Cod selection should match in order to adjust SNR as per Table 2. Consequently, Fig. 6, Fig. 8 and Table 2 show throughput enhancements for satellite systems. They also create a robust

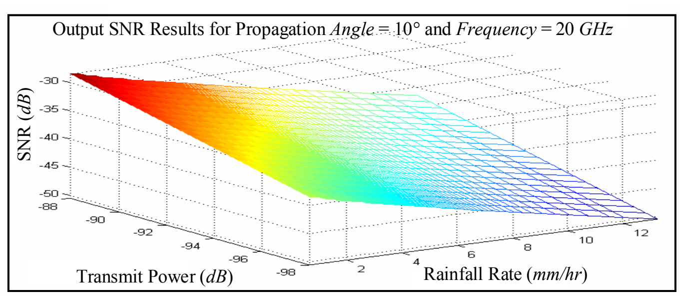


**Fig. 7.** Output SNR at Hazelton Station

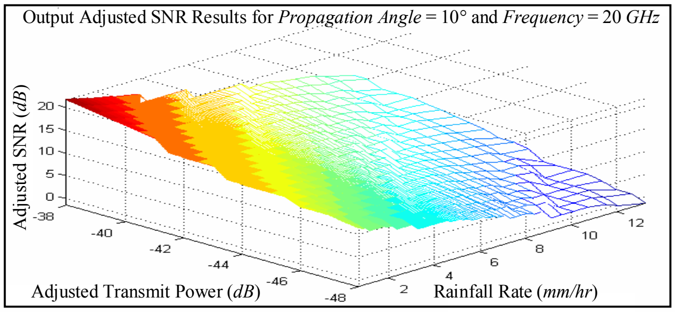


**Fig. 8.** Output adjusted SNR at Hazelton Station

system by allowing designers to work with flexible ranges by applying various combinations of modulation, coding and transmit power for any unpredicted weather conditions.

**Table 2.** Forward Link Modes and Performance for $\theta$=10 ℃ and $f$=30 *GHz*

| Modulation | LDPC Code Identifier | $E_s/N_0$ [dB] Measured and Estimated | Transmit Power [dB] | Rainfall Rate [mm/hr] |
|---|---|---|---|---|
| QPSK | 1/4 | -1.5 | -52 | 10.32 |
| QPSK | 1/3 | -0.3 | -51 | 10.03 |
| QPSK | 2/5 | 0.7 | -49 | 11.16 |
| QPSK | 1/2 | 1.3 | -50 | 9.31 |
| QPSK | 3/5 | 3.2 | -47 | 10.63 |
| QPSK | 2/3 | 3.8 | -48 | 8.91 |
| QPSK | 3/4 | 4.8 | -49 | 6.50 |
| QPSK | 4/5 | 5.3 | -46 | 9.29 |
| QPSK | 5/6 | 5.8 | -45 | 9.68 |
| QPSK | 8/9 | 6.8 | -44 | 9.97 |
| 8PSK | 3/5 | 6.4 | -42 | 12.71 |
| 8PSK | 2/3 | 7.3 | -43 | 10.48 |
| 8PSK | 3/4 | 8.6 | -41 | 11.25 |
| 8PSK | 5/6 | 10.0 | -40 | 10.86 |
| 8PSK | 8/9 | 11.4 | -39 | 10.42 |
| 16PSK | 2/3 | 9.6 | -42 | 8.97 |
| 16PSK | 3/4 | 10.9 | -38 | 11.94 |
| 16PSK | 4/5 | 11.8 | -40 | 8.79 |
| 16PSK | 5/6 | 12.4 | -37 | 11.49 |
| 16PSK | 8/9 | 13.7 | -35 | 12.25 |

## V. CONCLUSIONS

Signal attenuation caused by rain, gaseous, cloud, fog and scintillation attenuations limit satellite's QoS links and system availability that operate at frequencies above Ku band.

By implementing fuzzy logic algorithm QoS is improved by providing accurate estimates for different weather attenuations that leads to adjust SNR output in lieu of a wide range of rainfall rate and transmitted power, for any specific frequency, propagation angle, transmission rate, gain, and location.

This proposed method enhances back propagation-learning algorithm by computing attenuation periodically to iteratively tune the IS with returned SNR values and by activating the weighted Modulation/Codepoint optimal values, depending on actual or predicted weather conditions.

Hence, this mechanism gives designers the flexibility to apply various combinations of modulation, coding and transmit power for any unpredicted weather condition in order to maximize system throughput as well as QoS.

## ACKNOWLEDGMENTS

- Kalai Kalaichelvan and Rama Munikoti of EION, Bharat Rudra of OCE, and Derek Best of Precarn for supporting this project.
- Also, Andre Bigras, Abdul Lakhani and Mike Rosberg of Telesat for verifying the applicability and usefulness for satellite systems.

## REFERENCES

[1] K. Harb, A. Srinivasan, C. Huang and B. Cheng, "Prediction method to Maintain QoS in Weather Impacted Wireless and Satellite Networks", Proc. of the IEEE, SMC Conference, Montreal, QC, Canada, Oct. 2007.

[2] ITU-R, "Characteristics of precipitation for propagation modeling", Recommendation ITU-R P.837-4, 2001, P. Series Fascicle, Radio wave propagation, International Telecommunication Union, Geneva.

[3] ITU-R, "Specific attenuation model for rain for use in prediction methods", Recommendation ITU-R P. 838-3, 2003, P. Series Fascicle, Radio wave propagation, International Telecommunication Union.

[4] K. Harb, A. Srinivasan, C. Huang and B. Cheng, "QoS In Weather Impacted Satellite Networks", Proc. of the IEEE Pacific Rim Conference on Communications, Computers and Signal Processing, Victoria, B.C., Canada, Aug. 2007.

[5] R. K. Crane, "Prediction of the Effects of Rain on Satellite Communication Systems", Proc. of the IEEE, Vol. 65, No.3, pp. 456-474, March 1977.

[6] ITU-R, "Rain height model for prediction methods", Recommendation ITU-R P.839-3, 2001, P. Series Fascicle, Radio wave propagation, International Telecommunication Union, Geneva.

[7] A. Dissanayake, J. Allnutt, F. Haidara, "A prediction model that combines rain attenuation and other propagation impairments along Earth-satellite paths", IEEE Trans. on Antennas & Propagation, Volume 45, Issue 10, pp. 1546 – 1558, Oct. 1997.

[8] T. Boonchuk, N. Hemmakorn, P. Supnithi, M. Iida, K. Tanaka, K. Igarashi, Y. Moriya, " Rain Attenuation of Satellite link in Ku band at Bangkok ", Information, Communications and Signal Processing, Fifth International Conference, pp. 1093 – 1096, Dec. 2005.

[9] ITU-R, "Propagation data and prediction method required for the design of Earth-space Telecommunication systems", Recommendation ITU-R P.618-7, 2001, P. Series Fascicle, Radio wave propagation, International Telecommunication Union, Geneva.

[10] Garcia-Lopez, J.A. et al, (1988), " Simple Rain Attenuation Prediction Method for Satellite Radio Links," IEEE Trans. on Antennas & Propagation, Vol. 36, No. 3, March 1988.

[11] Karasawa, Y.T., & T. Matsudo, " Characteristics of fading on low-elevation angle Earth-space paths with concurrent rain attenuation and scintillation, " IEEE Trans. on Antennas & Propagation, Vol. 39, No. 5, pp. 657 – 661, May 1991.

[12] A. Safaai-Jazi, H. Ajaz, W. L. Stutzman, " Empirical models for rain fade time on Ku- and Ka-band satellite links ", IEEE Trans. on Antennas & Propagation, Vol. 43, No. 12, pp. 1411 – 1415, Dec. 1995.

[13] W. J. Vogel, J. Goldhirsh, " Multipath fading at L band for low elevation angle, land mobile satellite scenarios ", IEEE selected areas in communications, Vol. 13, No. 2, pp. 197 – 204, Feb. 1995.

[14] A. A. Aboudebra, K. Tanaka, T. Wakabayashi, S. Yamamoto, H. Wakana, " Signal fading in land-mobile satellite communication systems: statistical characteristics of data measured in Japan using ETS-VI ", IEEE Trans. on Microwave, Antennas & Propagation, Vol. 146, No. 5, pp. 349 – 354, Oct. 1999.

[15] E. Lutz, M. Werner, A. Jahn, *Satellite Systems for Personal and Broadband Communications*, pages 47-82. Springer, New York, 2000.

[16] K. Yasukawa, M. Yamada, Y. Karasawa, " Tropospheric scintillation in the 14/11-GHz bands on Earth-space paths with low elevation angles ", IEEE Trans. on Antennas & Propagation, Vol. 36, No. 4, pp. 563 - 569, April 1988.